Study of thermal flows from two-dimensional, upward-facing isothermal surfaces using a laser speckle photography technique

K. D. Kihm, S. K. R. Cheeti

Abstract A laser specklegram or speckle photography technique allows a direct measurement of surface temperature gradients and provides a full field interrogation with an extremely high resolution from a single data taking. The specklegram technique has been successfully applied to investigate the natural convection heat transfer from an upward-facing isothermal plate. For a plate with a large aspect ratio of 15, both local and global Nusselt numbers have been determined from the direct measurement of local temperature gradients. The Rayleigh number, based on the length scale equivalent to the ratio of the surface area to the perimeter, has been varied from 9.0×10^3 to 4.0×10^4. The present result for the global heat transfer has shown that a 1/5-power law, i.e., $Nu = C_1 Ra^{1/5}$, correlates the data more properly whilst previously published results showed a large scatter in the exponent, ranging from 1/8-power to 1/4-power. The proportional constant, C_1 has been determined to be 0.56 which shows a fairly good agreement with previously published theoretical results. The laser specklegram technique has shown a strong potential as a powerful and convenient method for an experimental assessment of natural convection heat transfer problems. The specklegram technique at the same time has eliminated the deficiencies of both the mass transfer analogy technique and the classical heat transfer measurement technique.

List of symbols

- a characteristic length scale defined as $a = A/P$ where A is the surface area and P is the perimeter of the plate edge [mm]
- AR aspect ratio [L/H]
- c defocusing distance [mm]
- d image distance of Young's fringes from speckle negative
- h thermal convection coefficient [W/m^2 ·K]
- ~~h~~ average thermal convection coefficient [W/ m^2 ·°C]
- H width of the test section measured perpendicular to the optic axis [mm]
- k thermal conductivity [W/m • K]
- L length of the test section measured parallel to the optical axis [mm]
- n index of refraction
- Nu local Nusselt number [ha/k]
- ~~Nu~~ global Nusselt number [ha/k]
- Pr Prandtl number [$\equiv \nu/\alpha$]
- q heat flux per unit area [W/m^2 ·s]
- Ra Rayleigh number $\left[\equiv \frac{g\beta(T_w - T_e)a^3}{\alpha\nu}\right]$
- s fringe spacing [mm]
- Sc Schmidt number [$\equiv \nu$/D]
- T temperature [K]

Greek symbols

- α thermal diffusivity [m^2/s]
- β volumetric coefficient of expansion [1/T$_\infty$)
- ν kinematic viscosity of air [m^2/s]
- λ wavelength of helium-neon laser [632.8 nm]
- Δ amount of speckle dislocation

1 Introduction

When an experiment for determining heat transfer coefficients is performed using conventional measurement techniques, which are typically based on either the mass transfer analogy of sublimation or on measurement of the electric power consumption of the surface foil heaters, it would not be easy to determine the local heat transfer coefficients with acceptable accuracy and resolution. One of the major reasons for the difficulties is because these conventional methods are not capable of directly measuring the wall temperature gradients. These techniques, instead, generally work in measuring global heat transfer coefficients. Besides, the heat/mass analogy technique does not provide a perfect analogy because of the nonzero diffusion velocity at the subliming surface which can overestimate the `analogous' heat transfer. On the other hand, use of the surface heater monitoring technique is not appropriate for natural convection problems where the portion of natural convection transfer out of the total heater power is small and extremely difficult to measure.

A laser specklegram technique or speckle photography (Merzkirch,1987,1989) is capable of directly measuring the local surface temperature gradients of heated surfaces. The specklegram technique provides an extremely high resolution for the evaluation of the local quantities, satisfactory measurement accuracy and full field information from a single speckle

Received: 13 *September 1993/Accepted: 7 March 1994*

K. D. Kihm, S. K. R. Cheeti
Department of Mechanical Engineering, Texas A&M University, College Station, Texas 77843-3123, U.S.A.

Correspondence to: K. D. Kihm

photograph. In the present work, the laser specklegram technique has been applied to carefully investigate the thermal flows around an upward-facing isothermal plate. The same problem has been studied previously in many different ways, but still under dispute, showing a wide scatter in their results of heat transfer correlation coefficients. The goals of the present study are twofold: (1) demonstration of the usefulness of the specklegram technique as a convenient and accurate tool to assess local and global heat transfer correlations for natural convection problems, and (2) determination of the heat transfer correlation for the case of two-dimensional natural convective flow from an upward-facing isothermal plate.

Goldstein and Lau (1983) presented an extensive review of both experimental and numerical studies of heat convections from horizontal heated surfaces with various configurations. Since the earliest known work that could be traced (Fishenden and Saunders, 1950), several studies in the earlier era (Bosworth, 1952, Mikheyev, 1968, Al-Arabi and El-Riedy, 1976) have investigated square and circular heated surfaces. The heat transfer behaviour has also been treated on a different premise using an electrochemical method (Wragg and Loomba, 1970, Lloyd and Moran, 1974) or a mass transfer analogy (Goldstein et al.,1973, Goldstein and Lau, 1983). Although the mass transfer analogy has certain advantages, it has a major drawback associated with the heat and mass transfer analogy. In the mass transfer experiments there exists a nonzero normal velocity at the plate surface, whereas such a surface velocity is not present in heat transfer problems. Nusselt (or Sherwood) numbers can be overestimated in the mass transfer analogy in comparison to its heat transfer counterpart. The discrepancy occurring because of the imperfect analogy will be more serious for natural heat transfer problems than in forced convection cases.

The measured data for the average Nusselt number were generally presented as a 1/4-Power or 1/5-power correlation, i.e., $Nu=C_1\,Ra^{1/4}$ or $C_2\,Ra^{1/5}$. The proportional constant C_1, ranged from 0.38 (Fishenden and Saunders, 1950) to 0.59 (Goldstein et al.,1973), and C_c from 0.746 (Goldstein and Lau, 1983) to 0.834 (Goldstein et al., 1973), depending on the tested *Ra* ranges. The shapes of surface studied were mostly square, occasionally circular (Al-Arabi and El-Riedy, 1976, Wragg and Loomba,1970, Lloyd and Moran, 1974, Goldstein et al., 1973), triangular (Lloyd and Moran, 1974), and rectangular with aspect ratios varying from 2.0 (Lloyd and Moran, 1974) up to 7.0 (Goldstein et al., 1973).

Optical visualization techniques, though to a limited extent, have been used to study the free convection heat transfer from a flat surface. The techniques include a semifocusing schlieren apparatus (Rotem and Claassen, 1969A), Machzender interferometry (Pera and Gebhart, 1973) and live fringe interferometry (Faw and Dullforce, 1981). These studies discovered the existence of laminar thermal boundary layers that were sometimes irregular and did not always separate at the same location.

Though the present work is experimental, it is relevant to have a brief account of the previous theoretical studies. For an infinitely long strip surface analyses were made using an integral method (Levy and Schenectady, 1955), a similarity solution of heat transfer (Rotem and Claassen, 1969B) and of mass transfer (Bandrowski and Rybski,1976), a perturbation method (Pera and 1983). These analytical and numerical results have predicted symmetrically developing thermal layers, which in turn implies the limited nature of the theoretical approach. All these studies yielded a 1/5-power correlation with C_1 varied from 0.5598 (Bandrowski and Rybski,1976) to 0.646 (Pera and Gebhart,1973) for $Pr = 0.72$.

More consistent data were obtained in the predictions than in the experiments, where different techniques applied for different surface configurations resulted in scattered values of C_1 and C_2 for different ranges of the Rayleigh numbers. The different surface configurations such as square and circular geometries could incorporate strong three-dimensional ambiguities and the different measurement techniques might have introduced different data biasing as a direct determination of the wall temperature gradient was not available. In order to alleviate these traditional problems, a high aspect ratio of 15 was considered for the present rectangular surface and the aforementioned laser specklegram technique was employed.

2 Experiments

The heat transfer phenomena of a solid surface with distributed heat sources can simulate many popular engineering problems, for example: cooling in electronic packaging, turbine blade cooling, and a variety of heat exchangers. Assuming a steady problem with uniformly distributed heat sources (Fig. i), such as a plate heater affixed to the solid base, the energy balance yields

$$q_s = q_r + q_k + q_z \tag{1}$$

where the subscripts *s, r, k, z* denote heat source, heat radiation, conduction losses, and heat convection, respectively. One typical measurement technique for heat convection involves setting the total heat generation, q_s, and then requires the determination of the heat radiation, q_r and the conduction losses, q_k, so that these latter two terms are subtracted from q_s to determine q_z. The whole experimental apparatus other than the test surface must be wrapped in bulky insulation material to minimize the losses to the environment, which are not easy to estimate accurately. The uncertainties in determining the radiation heat losses are equally difficult to quantify. In fact, radiation heat loss is usually neglected. Incorrect evaluation of the conduction and radiation losses can significantly affect the measurement accuracy, especially for natural convection problems where the amount of heat loss could be as much as the amount of heat convected.

All these difficulties can be avoided if the heat transfer coefficient, *h,* can be directly measured without involving the total heat generation rate. Taking account of the energy balance adjacent to the heated surface gives:

$$q_z = h\,(x, y)\,(T_w - T_e) = -k\,(dT/dy)_w \quad \text{or}$$
$$h(x, y) = -k(dT/dy)_w\, l\,(T_w - T_e) \tag{2}$$

where the subscripts *w* and *e* denote the wall and the environment, respectively. When the thermal conductivity of the environmental fluid, and the wall and the environmental temperatures are known or measured, the heat transfer coefficient is determined from the measurement of the wall temperature gradient. The laser specklegram technique allows

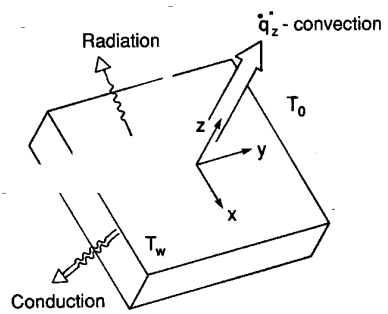

Fig. 1. Convection, conduction and radiation heat transfers from a solid surface with distributed heat sources

direct and nonintrusive measurements of the wall temperature gradient, $(dT/dy)_w$.

2.1
Laser speckle photography technique

Optical speckles are generated as a result of the random intensity distribution of light when a highly coherent, collimated and monochromatic light beam, such as a laser, is scattered by a rough surface. The speckle formation through the granular surface of a ground glass is schematically illustrated in Fig. 2. Without a presented test section, the light rays form speckles (bright or dark spots) on any arbitrary plane beyond the ground glass. When a test section is presented, the light rays refract at a small angle because of the variable density field of the test section, and form speckles at different location on the same arbitrary plane. A specklegram is taken by photographically superimposing both speckles formed with and then without the test section. The resulting speckle photograph carries the information on the amount of speckle dislocation.

By considering the optical arrangement of the specklegram technique (Fig. 3) one can derive an expression for the magnitude of the temperature gradient as (Kastell et al., 1992):

$$|dT/dy| = A\Delta(dn/dT)^{-1}\, Lc \qquad (3)$$

where A represents a group of optical and geometrical parameters, Δ denotes the amount of speckle dislocation and n is the refractive index of the medium. L is the length of a test section measured along the optic axis, and c is called a 'defocusing' length measured from the ground glass to the speckle plane. The image of the test

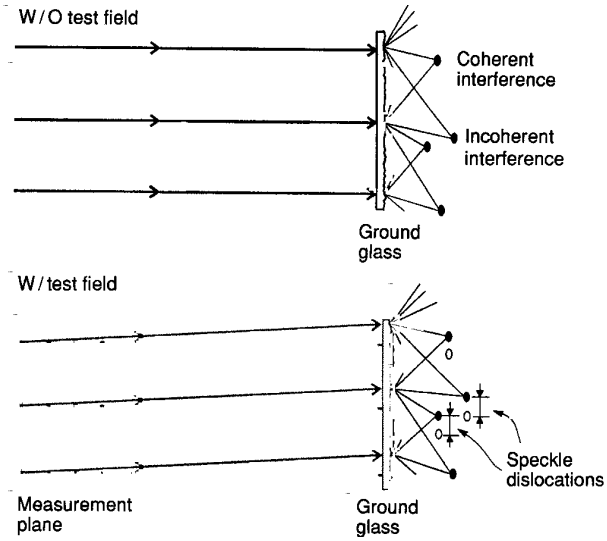

Fig. 2. A schematic illustration of optical speckle formation and dislocation

section is focused onto the ground glass whereas the camera captures the test section image formed on the speckle plane. The distance between the two locations, the ground glass and the speckle plane, is called a defocusing length. It is necessary to maintain the defocusing length minimal, yet long enough for distinctive recording of speckle dislocations. A defocusing distance of 25 mm was used for all the present measurements. The temperature dependence of the refractive index of air at 632.8 nm wavelength of He-Ne laser is given as (Vest, 1979):

$$dnldT = 1.075\times 10^{-6}/(1 + 0.00368184\ T)^2 \qquad (4)$$

where T is in degrees Celsius and is taken to be equal to the wall temperature. The present specklegram system has two 318 mm diameter parabolic mirrors of 1,911 and 2,553 mm focal length, respectively. These mirrors are represented by lens symbols for convenience in Fig. 3. It was shown that the longer focal length can effectively enhance the overall signal-to-noise ratio of the system (Kihm,1992). A 4-inch-by-5-inch format bellows camera was used to record specklegrams on Kodak No. 4415 Technical Pan 4 × 5 Format ASA 400 negative film. The aperture setting of the camera was F=5.6 which was the widest opening of the Nikon f= 210 mm lens of the bellows camera.

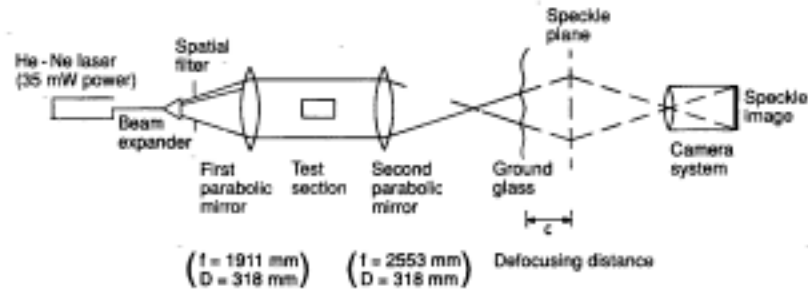

Fig. 3. An optical train of the specklegram system

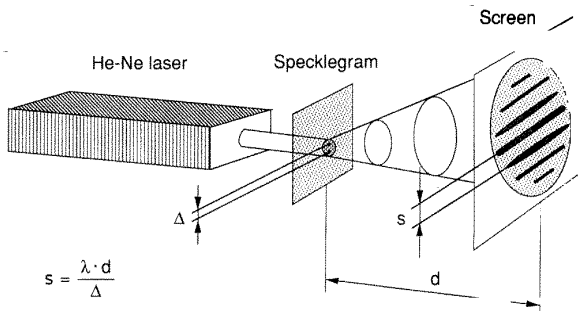

Fig. 4. A schematic illustration of Young's fringe construction for the data reduction of speckle photography

The amount of speckle dislocation is determined indirectly from the principle of Young's fringes (Hecht, 1987). Young's fringes are constructed by illuminating the specklegram with a smaller 5 mW He-Ne laser (Fig. 4). A beam expander/collimator reduces the 0.8 mm nominal beam diameter down to 0.4 mm diameter. The fringes are then digitized using a CCD camera and the fringe spacing is measured with PC software that identifies the darkest locations between fringes. The fringe spacing, s, and the speckle dislocation, Δ, have a relationship:

$$s = \lambda d \, l \, \Delta \tag{5}$$

where λ denotes the wavelength of the laser and *d is* the distance between the specklegram negative and the image plane of the Young's fringes. Once the fringe spacing, s, is measured, the heat convection coefficient, h, can be determined by substituting Eqs. (3), (4) and (5) into (2):

$$h(x,y) = \frac{Ak\lambda dLc}{s(T_w - T_e)}\left(\frac{dn}{dT}\right)^{-1} \tag{6}$$

Narrower fringes are constructed when the temperature gradient is high and the speckle dislocation is large. Conversely, thicker fringes are formed when the temperature gradient is low. The fringes are formed perpendicular to the major heat transfer direction, parallel to the statistically dominating direction of the speckle dislocations. If the fringe spacing is evaluated at the solid boundary, the wall temperature gradient and heat convection coefficient are readily determined.

One of the best features of the specklegram technique is that a single speckle photography provides a full field interrogation of a test field, and at the same time can eliminate temporal inconsistency that is unavoidable for scanning a measurement probe in the case of classical techniques such as a thermocouple probe. In comparison with interferometry techniques, the major advantages of the specklegram technique are its higher data resolution with enhanced accuracy and relatively lower sensitivity to external vibrations (Shu and Li, 1993). The initial cost of an interferometry system is too high and proper mounting is required to absorb any vibrations, whereas the speckle holography system significantly alleviates both the cost and the sensitivity problems.

The specklegram system has been successfully applied for various natural convection problems occurring in vertical channel flows (Kastell et al., 1992, Wernekinck and Merzkirch, 1986) and in converging channel flows (Kihm et al., 1993). The results in these studies demonstrated high accuracy and convenience, and showed good agreement with previous calculations and data. The error analysis has been carried out fox the present condition using the root-sum-square method recommended by Kline and McClintock (1953). The analysis with a typical estimate of the uncertainty for each parameter shows errors of 5.79% for the wall temperature gradient values. For most conditions, a typical 5% error is expected.

2.2
Horizontal isothermal plate

A horizontal isothermal plate was constructed to simulate the heat transfer behaviour, for example, for the convective flow above a horizontally placed electronic element such as a memory chip or a board. Figure 5 shows a cutaway view, perpendicular to the optic axis, of the horizontal isothermal plate. The heated surface had a large aspect ratio of 15, 40 mm wide and 600 mm long, and the 600 mm long side was oriented parallel to the optic axis. The main criterion for the high aspect ratio for the heated plate was to simulate a two-dimensional heat transfer behaviour from a horizontal heated plate. In principle, this goal would be achieved only with infinite aspect ratio, but a plate of infinite aspect ratio is impossible to build. The 15 : 1 ratio was assumed large enough to satisfy the twodimensionality.

Two strips of 15 mm wide and 25.4 μm thick stainless steel foil were connected in series and were mounted side by side using a double-stick tape on the wooden base block. A series circuit was established by soldering the foils to a copper bus bar at one end of each foil strip. The heater strips were then covered with a single piece of 127 μm thick stainless steel shim metal to ensure a smooth surface which was required for speckle photography. The surface plate and the foil heater strips were glued together using an electrically nonconducting but thermally conducting double-stick tape. The entire heated plate was mounted on a tripod for appropriate levelling and positioning. Twenty-two evenly spaced T-type thermocouples were soldered along the centreline, all along the length of the surface plate from underneath. The longitudinal variations of the thermocouple reading is negligibly small, showing ± 0.1 °C.

The surface temperature was taken as a constant temperature value spanning the central 95% of the heated plate width of 40 mm. The spanwise surface temperature was occasionally monitored by scanning a thermocouple probe along the width

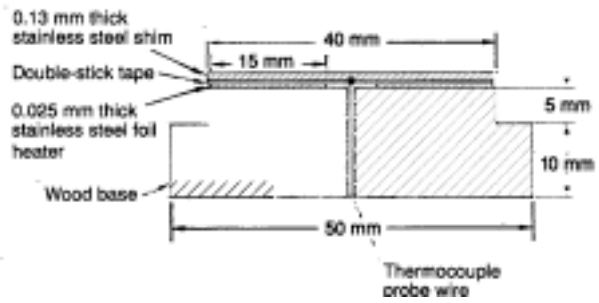

Fig. 5. Cutaway view of the horizontal isothermal plate

at various axial locations. Within the central 95% of the span, the temperature readings showed excellent consistency with less than ± 2% variations. Slight temperature decreases were detected outside the central 95% towards both edges since a larger heat transfer occurred by the induced upward wind of cold air. The amount of temperature decrease near the edge was less than to% of the central value and the overall temperature profiles represented an isothermal surface condition fairly well.

Results and discussion

For the case of an upward facing heated surface, less dense fluid forms on the top surface and its tendency to rise is inhibited by the denser, cooler fluid which is moving downwards (Fig. 6). The thermal plume, therefore, is unstable in nature. Although not presented, an extensive observation using a schlieren visualization method revealed that the plume did not always develop exactly at the centre. The asymmetry in the surface heat transfer was largely enhanced with increasing surface temperature ($Ra > 3 \times 10^4$), and the thermal layer became very irregular and distorted in shape. This increased flow fluctuation is attributed to the transition of laminar to turbulent flow.

Results are presented in two different dimensionless numbers, Nusselt and Rayleigh numbers. The characteristic length, a, was taken to be the ratio of the surface area to the perimeter (a=18.7 mm for the present case). Fifteen different temperature conditions were studied and the Rayleigh number

$$\left(Ra \equiv \frac{g\beta(T_w - T_e)a^3}{\alpha\gamma} \right)$$ is ranged from 9×10^3 to 4×10^4. For each Ra, the measurement was repeated three times, and the averaged amount of speckle dislocations (or the fringe spacings) was used to determine the local heat transfer coefficient of Eq. (6). The global heat transfer coefficient was determined by the spatial integration of the local data across the plate width. The number of local data points for the integration was doubled starting from five until the resultant global Nusselt number approached an asymptotic value. For most cases, io data points across the 40 mm width were sufficient to reach a constant global Nusselt number within 2 or 3a/o of the successive calculation with 2o data points.

Figure 7 presents Young's fringes for three different cases of Ra=9.74 x io' (Fig. 7a), 2.35 x io' (Fig. 7b) and 3.65 x to' (Fig. 7c). The number above each inset photo represents the local Nusselt number at the solid surface. The image of the surface will

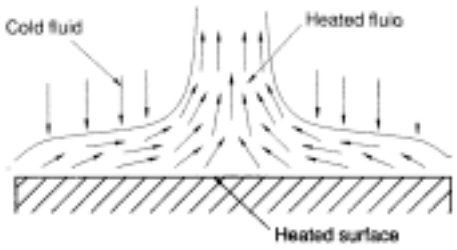

Fig. 6. Thermal flow of natural convection from an upward-facing heated plate

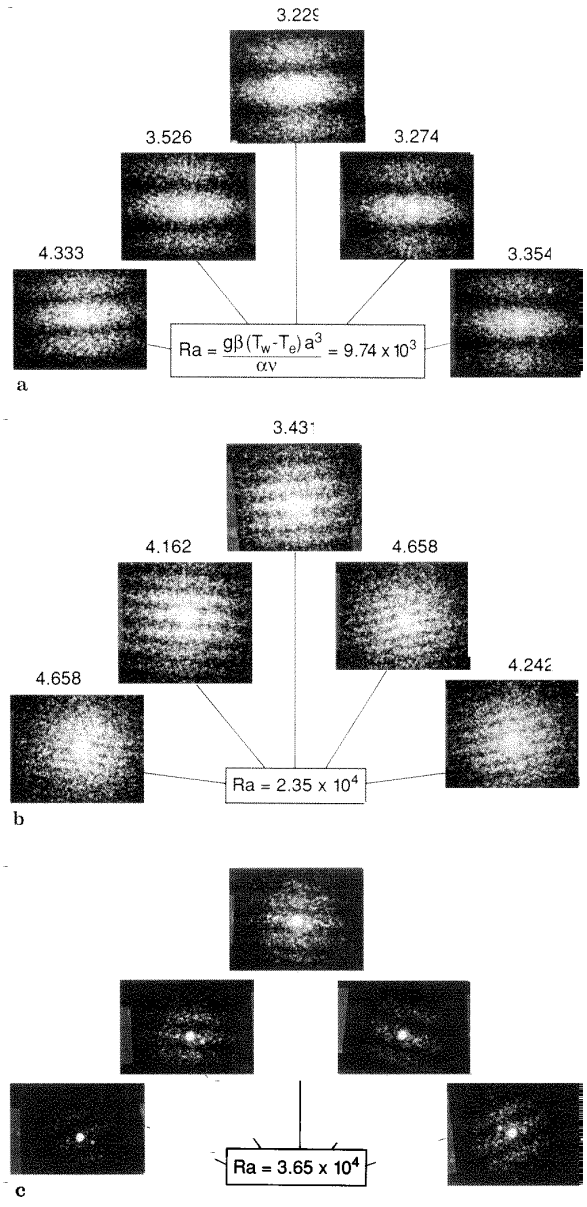

Fig. 7a-c. Distribution of the speckle fringes and the local Nusselt numbers across the heated surface in perpendicular to the optic axis for three different Rayleigh numbers. a Ra=9.7 × 10^3, b Ra=2.35 × 10^4 and c Ra=3.65 × 10^4

image blur. For the present condition, the image blur was estimated to be less than 0.5 mm on a physical scale. Taking one half of this amount as a closest location for fringe construction, the surface temperature gradient measurement was made with 250 μm spatial uncertainties.

For higher Rayleigh number, the speckle dislocation, Δ, increases because of the larger temperature gradient [Eq. (3)] and the fringe spacing is narrower [Eq. (5)]. For the lower Rayleigh number, all the fringes are nearly horizontally oriented showing that the convection heat transfer occurs in the normal direction across the heated surface. This case also accompanies

a fairly uniform distribution of the local Nusselt number. For the case of the intermediate Rayleigh number (Fig. 7b), both orientation and spacing of the fringes vary slightly across the surface indicating that the convective flow from the heated surface is fluctuating somewhat in both its direction and magnitude. It is expected that more aggressive convection occurs along the perimeter where direct contact is made between the hot plate and the cold air convecting upward. This results in higher Nusselt numbers near both edges than in the middle. The asymmetry of Nusselt number distributions is enhanced compared with the previous case of lower *Ra*.

The flow becomes quite unstable at the high *Ra* (Fig. 70 and the fringe orientations are irregular showing poor repeatability from measurement to measurement. The widened fringe spacings, even with increased *Ra*, are misleading since the speckle photographs could have been taken under a severe influence of the beam steering due to the thermal flow fluctuations. As a result of this, individual speckles are enlarged and the apparent amount of speckle dislocation is reduced. The resulting local Nusselt numbers are underestimated and this indicates the limitation of the present speckle photography system.

The global Nusselt number averaged over the heated surface width has a power law correlation with Rayleigh number, i.e., $Nu = C_1 Ra^{c2}$. The global Nusselt numbers are presented for fifteen different Rayleigh numbers in Fig. 8. Each symbol represents an average of three independent measurements for the same Rayleigh number. The top dashed line represents the experimental data using an electrochemical method for $Sc = 2300$ (Wragg and Loomba, 1970), and the double-dotted line represents the result of the heat transfer measurement for the case of $Pr = 0.7$ (Fishenden and Saunders, 1950). The other experimental correlations discussed in the introduction were not appropriate for comparison since their *Ra* ranges were either too large or too small compared with the present Rayleigh number range. The solid curve represents the predictions using a perturbation method for $Pr = 0.72$ (Pera and Gebhart, 1973), and the bottom dashed line represents the similarity solution for mass transfer for the case of $Sc = 2.5$ and surface molar fraction of 5×10^{-4} (Bandrowski and Rybski, 1976). These two predictions represent the upper and lower limits of the reviewed family of theoretical results.

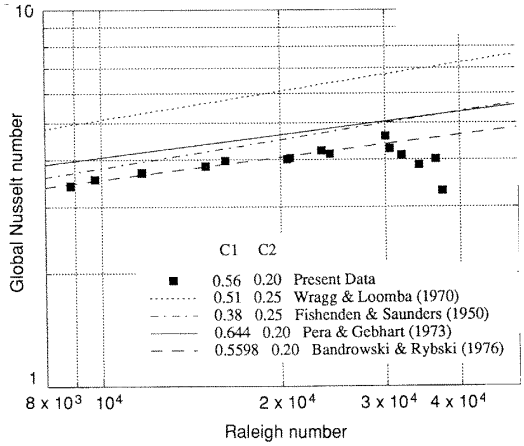

Fig. 8. Global Nusselt number versus Rayleigh number

The present data stay well within the range between the upper and the lower limit of the theoretical results up to $Ra = 3 \times 10^4$. C_1 and C_2 for the present case were determined to be 0.56 and 1/5, respectively. A 1/5-power law is shown to be more appropriate for both predictions and the present experiment, where two-dimensional flows were considered. Most previous data obtained from mass transfer analogy generally showed higher Nusselt numbers than the predictions and than the present data. The primary reason for this may be explained by introducing the concept of "specific perimeter per unit surface area", which is defined as the ratio of the perimeter to the surface area, i.e., the reciprocal of the characteristic length, a. Near the perimeter of the heated surface the heat transfer rate will be higher than that on the inner surface area because of the larger temperature differences between the surface and the upcoming cold air. The global Nusselt number, therefore, is expected to increase with increasing specific perimeter. The square or circular surfaces considered in the experiment (Wragg and Loomba, 1970) have a specific perimeter of $4/H$, where H denotes the length dimension of the square or the diameter of the circle. The present geometry ($40 H \times 600$L mm surface) provides a specific perimeter of $2.13/H$ and the infinitely long surface of width H considered in the theoretical studies is equivalent to a specific perimeter of $2/H$. The global Nusselt number shows a fairly consistent increase with increasing specific perimeter of the heated (or sublimed) surfaces. An additional reason for the overestimation of the previous data can be attributed to the limitation of the mass or electrochemical analogies with nonzero velocity at the surface. The data from the direct heat transfer experiment by Fishenden and Saunders (1950) do not show such a large discrepancy when compared with the present data.

The upper side of the cylinder may be considered rather similar to a horizontal plate. However, the additional contribution from the lower half of the cylinder should result in a significantly higher amount of heat transfer. Heat transfer from horizontal cylinders for the Rayleigh number ranging from 10^4 to 10^9 may be calculated from $Nu = 0.53\, Ra^{0.25}$ (Hyman et al., *1953).* The exponent has a higher value than the present *0.2* and the proportional constant is larger than *0.51* of the highest correlation by Wragg and Loomba *(1970).* Heat transfer from horizontal cylinders is noticeably higher than that from an upward-facing isothermal plate.

Also noteworthy in Fig. 8 is that for $Ra > 3 \times 10^4$ the present data start to deviate significantly from the prediction range. It is believed that the deviation is due to the transition from laminar to turbulent flow. Turbulent fluctuations of thermal flow will steer the laser beam and result in blurred or oversized speckles, which in turn contribute to reduce the speckle dislocation amount by more than it actually should be. This underestimation of Nusselt numbers is especially true when the speckle recording time, or equivalently, the camera shutter speed is relatively long compared with the flow fluctuating time scale. The present specklegram system used a *35* mW helium-neon laser and the specified laser light intensity limited the camera shutter speed to no faster than *1/125* s, which can be longer than typical fluctuating time scales in the transition from laminar to turbulent flows. The critical *Ra* for the transition in air has

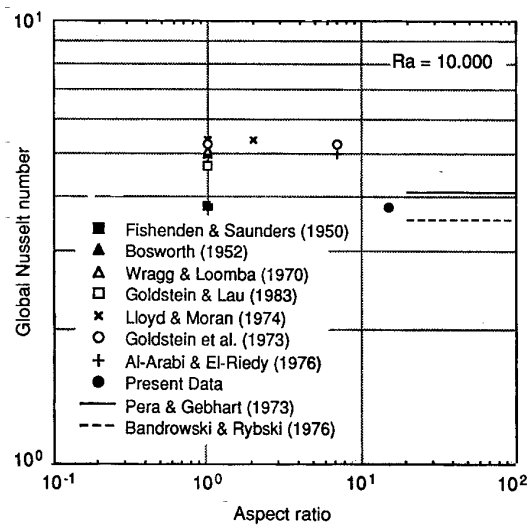

Fig. 9. Global Nusselt number versus aspect ratio for $Ra = 10^4$

been found to be widely ranged from 3.8 x 10^4 (Ishiguro et al. 1978) to 7 x 10^5 (Rotem and Claassen, 1969A). The initiation of the transition was found to be as low as lo', based on the experimental study using a mass transfer analogy (Goldstein and Lau, 1983).

Finally, an attempt was made to explore an effect of the aspect ratio (AR) of the heated surface on the global Nusselt number, and the *Ra* ranges of previous experimental correlations were extended up or down to meet the present range. Figure 9 presents the global Nusselt number of $Ra=10^4$ for different aspect ratios. Most previous experiments were performed for square or circular geometries (AR = 1.0) and the corresponding data are widely scattered. Only a few cases of rectangular surface have been studied up to AR of 7.0 to date, but no apparent dependence of the correlation on the aspect ratio has been observed. For the present case of AR =15.0, the Nusselt number approaches the theoretical values that were obtained for infinite aspect ratio. Although further experimental substantiation is needed, it is expected that the global Nusselt number will gradually decrease with increasing aspect ratio because of the decrease in the specific perimeter per unit area.

4 Conclusions

A laser specklegram technique has been successfully applied to measure both local and global Nusselt numbers for the laminar convective flow from horizontal isothermal surfaces. In order to use the technique for turbulent flows, a significantly shorter speckle recording time, one much shorter than the turbulent fluctuating time scale, must be achieved. One way to accomplish this would be to replace the He-Ne laser with a more powerful laser such as an Argon-Ion or a pulsed Nd:YAG laser.

Three fundamental conclusions follow from the present investigation:

(1) The laser specklegram technique is proven not only to be a convenient but also very accurate means of heat transfer measurement, especially for the laminar natural convection problems.

(2) The convective heat transfer from the horizontal isothermal surface shows an increase with increasing "specific perimeter per unit surface area", or with decreasing aspect ratio of the heated surface.

(3) The 1/5-power law has been determined, i.e., Nu =C_2 $Ra^{1/5}$, where the coefficient C_2 has been estimated to be approximately 0.56 for a rectangular plate with an aspect ratio of 15.

References

Al-Arabi A; El-Riedy MK (1976) Natural convection heat transfer from isothermal horizontal plates of different shapes. Int J Heat Mass Transfer 19: 1399-1404

Bandrowski J; Rybski W (1976) Free convection mass transfer from horizontal plates. Int J Heat Mass Transfer 19: 827-838

Bosworth RLC (1952) Heat transfer phenomena. PP 102-104. New York: John W iley

Faw RE; Dullforce TA (1981) Holographic interferometry measurement of convective heat transport beneath a heated horizontal plate in air. Int J Heat Mass Transfer 24: 859-869

Fishenden M; Saunders OA (1950) An introduction to heat transfer. 95-97. London: Oxford Univ Press

Goldstein RJ; Lau K-S (1983) Laminar natural convection from a horizontal plate and the influence of plate-edge extensions. J Fluid Mech 129: 55-75

Goldstein RJ; Sparrow EM; Jones DC (1973) Natural convection mass transfer adjacent to horizontal plates. Int J Heat Mass Transfer 16: 1025-1035

Hecht E (1987) Optics (2nd ed.). PP 339-346. Reading: Addison Wesley

Hyman SC; Bonilla CF; Ehrlich SW (1953) Heat transfer to liquid metals from horizontal cylinders. AIChE Symp Heat Transfer, Atlantic City, 21

Ishiguro R; Abe T; Nagase H; Nakanishi S (1978) Heat transfer and flow stability of natural convection over upward-facing horizontal surfaces. Proc 6th Intl Heat Transfer Conf 2: 229-234

Kastell D; Kihm KD; Fletcher LS (1992) Study of laminar thermal boundary layers occurring around the leading edge of a vertical isothermal wall using a specklegram technique. Exp Fluids 13: 249-256

Kihm KD (1992) Image blurring of test section boundary in a specklegram technique for temperature gradient measurements. Appl Opt 31: 5907-5910

Kihm KD; Kim JH; Fletcher LS (1993) Investigation of natural convection heat transfer in converging channel flows using a laser specklegram technique. J Heat Transfer 115: No. 1, 140-148

Kline SJ; McClintock FA (1953) Describing uncertainties in single sample experiments. Mechanical Engineering, Vol 75, January

Levy S; Schenectady NY (1955) Integral method in natural convection flow. J APPl Mech 77: 515-522

Lloyd JR; Moran WR (1974) Natural convection adjacent to horizontal surface of various planforms. J Heat Transfer 96: 443-447

Merzkirch W (1987) Flow visualization (2nd ed.). 152-158. New York: Academic Press

Merzkirch W (1989) Speckle photography. In: Handbook of flow visualization (ed. Yang W-J). 181-187. New York: Hemisphere

Mikheyev M (1968) Fundamentals of heat transfer. 77-78, Moscow: Peace Pub

Pera L; Gebhart B (1973) Natural convection boundary flow over horizontal and slightly inclined surfaces. Int J Heat Mass Transfer 16: 1131-1146

Rotem Z; Claassen L (1969A) Natural convection above unconfined horizontal surfaces. J Fluid Mech 38: 173-192

Rotem Z; Claassen L (1969B) Free convection boundary-layer flow over horizontal plates and disks. Canadian J Chem Eng 47: 461-468

Shu JZ; Li JY (1993) A laser schlieren-speckle interferometry system for measurement of phase objects. J of Flow Visualization and Image Processing 1: 63-68

Vest CM (1979) Holographic interferometry. 344-345. New York: John Wiley & Sons

Wernekinck U; Merzkirch W (1986) Measurement of natural convection by speckle photography. In: Heat transfer (eds. Tien CL; Carey VP; Ferrell JK). 531-535. Washington: Hemisphere

Wragg AA; Loomba RP (1970) Free convection flow patterns at horizontal surfaces with ionic mass transfer. Int J Heat Mass Transfer 113: 439-442